

3-Aminopropyltrimethoxysilane mediated synthesis of Gold Nanoparticles and its Multimetallic analogue



Thesis submitted in partial fulfillment for the
Award of degree

Doctor of Philosophy

By

Gunjan Pandey

DEPARTMENT OF CHEMISTRY
INDIAN INSTITUTE OF TECHNOLOGY
(BANARAS HINDU UNIVERSITY)
VARANASI- 221005
INDIA

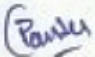
Roll No. 13051001

October 2016

CERTIFICATE

It is certified that the work contained in the thesis titled "*3-Aminopropyltrimethoxysilane mediated synthesis of Gold Nanoparticles and its Multimetallic analogue*" by "*Gunjan Pandey*" has been carried out under my supervision and that this work has not been submitted elsewhere for a degree.

It is further certified that the student has fulfilled all the requirements of Comprehensive, Candidacy and SOTA.


P. C. Pandey
(Professor)
Department of Chemistry
Indian Institute of Technology (BHU)
Banaras Hindu University,
Varanasi-221005

DECLARATION BY THE CANDIDATE

I, **Gunjan Pandey** certify that the work embodied in this thesis is my own bonafide work and carried out by me under the supervision of **Prof. P. C. Pandey** from **July 2013 to October 2016** at the **Department of Chemistry, Indian Institute of Technology, Banaras Hindu University, Varanasi**. The matter embodied in this thesis has not been submitted for the award of any other degree/diploma. I declare that I have faithfully acknowledged and given credits to the research workers wherever their works have been cited in my work in this thesis. I further declare that I have not willfully copied any other's work, paragraphs, text, data, results, etc., reported in journals, books, magazines, reports, dissertations, thesis, etc., or available at websites and have not included them in this thesis and have not cited as my own work.

Date: 25/10/2016 *Gunjan Pandey*
Place: Varanasi (Gunjan Pandey)

Certificate by the Supervisor

It is certified that the above statement made by the student is correct to the best of my knowledge.

Wade
25/10/16
विभागाध्यक्ष / HEAD
रसायन विज्ञान विभाग
Department of Chemistry
भारतीय प्रौद्योगिकी संस्थान (का.हि.वि.वि.)
Indian Institute of Technology (B.H.U.)
वाराणसी-221005 / Varanasi-221005

(Pandey)
Prof. P. C. Pandey
Department of Chemistry
Indian Institute of Technology (BHU)
Varanasi-221005

COPYRIGHT TRANSFER CERTIFICATE

Title of the Thesis: 3-Aminopropyltrimethoxysilane mediated synthesis of Gold Nanoparticles and its Multimetallic analogue

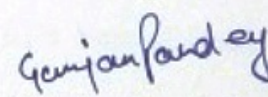
Name of the Student: Gunjan Pandey

Copyright Transfer

The undersigned hereby assigns to the Indian Institute of Technology (Banaras Hindu University) Varanasi all rights under copyright that may exist in and for the above thesis submitted for the award of the "*Doctor of Philosophy*".

Date: 25/10/2016

Place: Varanasi


(Gunjan Pandey)

Note: However, the author may reproduce or authorize others to reproduce material extracted verbatim from the thesis or derivative of the thesis for author's personal use provided that the source and the Institute's copyright notice are indicated.

ACKNOWLEDGEMENT

At the very beginning, I bow my head and offer flowers of reverence to "Mahamana" the late **Pt. Madan Mohan Malviya**, the founder of Banaras Hindu University, for his lifetime sacrifice and efforts in establishing such a great temple of learning for the cause of millions of students like me.

I would like to take this opportunity to express my gratitude to **Prof. P. C. Pandey**, who not only suggested me the research problem, but provided stimulating inspiration, valuable suggestions, appurtenant criticism, and showed a keen interest during the course of the study. My acknowledgements are also due to the **Prof. M. A. Quraishi**, former Head, Department of Chemistry, IIT (BHU) and **Prof. R. B. Rastogi**, Head, Department of Chemistry, IIT(BHU) for providing me the facilities of the department. I also express my gratitude to my RPEC members **Prof. Y. C. Sharma**, chemistry department and **Prof. Rajeev Prakash**, School of Material Science and Technology for their valuable suggestions. My warm thanks to the members of central instrumentation facility center (CIFC), departmental library, and the office staff of the chemistry department for their help and support.

I express my grateful thanks to my seniors **Dr. Arvind Prakash**, **Dr. Ashish Kumar**, **Dr. Richa Singh** and **Digvijay Panday** for their active and appreciative suggestions. A lot of thanks to my colleagues **Kalyani**, **Alka**, **Madhu** (SMST), **Shraddha**, **Shubhangi** and **Shwarnima** for their help and consistent support.

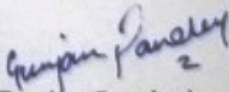
I would like to acknowledge UGC and MHRD, Government of India, for providing financial assistance (JRF, SRF and contingency).

I am grateful to my paternal grandparents, **Shri Laxmi. K. Pandey & Smt. Sonmati Pandey** and my maternal grandparents, **Shri Indra D. Tiwari (late) and Smt. Ram K. Tiwari (late)** for their constant blessings without which this thesis would not have been possible. I express my hearty indebtedness to my mother **Mrs. Usha Pandey** and father **Mr. Vimal K. Pandey** for their everlasting affection, encouragement, patience and substantial help throughout my life. I feel pleasure in expressing my heartfelt thanks to my elder brother **Mr. Ajit Vikram Pandey** and my elder sister **Mrs. KumKum Pandey** who inspired me to achieve the best in life in the form of higher studies.

I thank my mother-in-law, Late **Mrs. Meera Devi** and my father-in-law **Mr. Vikrama Pandey** for the encouragement throughout my Ph.D. tenure. I feel pleasure in expressing my heartfelt thanks to my brother-in-law **Mr. Sarsaswa Pandey** and my sister-in-law **Mrs. Sapna Pandey, Mrs. Kiran Pandey** and **Mrs. Ratan Dubey** for their support. A lot of thanks to youngsters in the family **Priya, Prashant, Nishant, Pallavi, Shivani, Rudra, Gauravi, Aditya, Soni, Lucky, Aadya, Rudransh, Darsh, Harsh, Utkarsh, Ribhu, Rishabh** and **Chhoti** for their constant support and love at each and every step.

At last, but not the least, deep appreciation is extended to my husband **Dr. Dhananjay K. Pandey** for his continued and unfailing love, support and understanding that has been a constant source of encouragement for the successful completion of this thesis.

Place: Varanasi
Date: 25/10/2016


(Gunjan Pandey)

PREFACE

Extensive use of colloidal gold in the field of sensing, therapeutics and catalysis is due to the unique physical and chemical properties they possess, that has led to a surge in its synthesis protocols. There are several techniques available for the synthesis of AuNPs, like Turkevich, Brust-schiffrin and Martin methods. However, such conventional methods have few limitations; (i) generally the AuNPs are produced as aqueous suspension (Turkevich method) and the use of such NPs in organic solvent causes agglomeration. Similarly, the AuNPs having compatibility with organic solvent (Brust- Schiffrin method) are not compatible in aqueous system; (ii) The AuNPs fabricated through conventional routes are generally produced as dilute solution i.e. the initial concentration of AuNPs precursor (Au^{3+}) is very low; (iii) Attempt to convert the homogenous suspension of AuNPs to heterogeneous matrix by adsorbing over some solid support (TiO_2 , Al_2O_3 etc.) causes an increase in size of the AuNPs or undergo agglomeration. Thus, there is a need to devise a method that can produce stable, concentrated colloidal suspension of AuNPs with the ability to convert from homogeneous suspension to heterogeneous catalyst (in powder form or as thin film) without compromising the catalytic behavior. This constitutes the theme of the present thesis work involving the active participation of functional alkoxy silanes which has shown its potentiality in yielding novel nanostructured material.

Functional Alkoxy silanes like 3-Glycidoxypropyltrimethoxysilane (3-GPTMS), 3-Aminopropyltrimethoxysilane (3-APTMS), epoxy cyclohexyltrimethoxysilane, trimethoxysilane etc. have been used for the synthesis of nanomaterials through sol-gel

process. Some of these alkoxysilanes have behaved as a potential reducing agent for PdCl_2 allowing the introduction of Pd within nanostructured network of organically modified silicates. Such findings established the role of functional alkoxysilanes (3-APTMS and 3-GPTMS) as reducing agent of noble metal ions and led the way for the use of such functionality during the synthesis of AuNPs and its multimetallic analogue. 3-APTMS capped noble gold ion can be precisely converted to AuNPs in the presence of another alkoxysilane 3-GPTMS or variety of organic reducing agents (THF-HPO, cyclohexanone, formaldehyde, acetaldehyde, acetone, t-butylmethylketone), thus controlling the dispersibility of as made NPs in variety of solvents covering wide range of polarity index. The study has been further extended to the 3-APTMS mediated synthesis of bimetallic (AuPd) and trimetallic (AgAuPd) NPs. 3-APTMS used for the synthesis of AuNPs have following properties: (i) 3-APTMS is **amphiphilic** in nature. Thus, the NPs made using 3-APTMS can be dispersed or fabricated in organic as well as aqueous solvents (ii) The reversible **imine** (-C=N-) linkage formed between amine group of 3-APTMS and organic reducing agent like formaldehyde (-C=O) during AuNPs synthesis has a great propensity to play attractive role in the synthesis of AuNPs. (iii) The 'trimethoxysilyl' group [-Si(OMe)₃] of 3-APTMS can be utilized for the conversion of homogenous nanoparticle suspension to **heterogeneous** solid matrix without addition of any external support like TiO_2 . The trimethoxysilyl group can also be utilized for casting film of the nanomaterial through sol-gel processing.

These considerations, inter alia, prompted me to take up the present work. The thesis is organized into seven chapters with 'Summary and Future Projection' at the end. Chapter (I) 'General Introduction' reviews the current status of the subject and gives the reasons for

embarking upon the present study. Chapter (II) deals with the synthesis and dispersibility of the AuNPs synthesized using 3-APTMS and 3-GPTMS where the synthesized AuNPs were dispersible in organic solvents at all concentration of 3-APTMS and 3-GPTMS while dispersibility in water required low concentration of either 3-APTMS or 3-GPTMS. Chapter (III) explores the suitability of THF-HPO as reducing agent with 3-APTMS to form the AuNPs in aqueous medium. Imine linkage (Organic-inorganic hybrid) formed between 3-APTMS and GBL assists AuNPs in displaying peroxidase mimetic ability as the linkage is catalytic in nature. The improved dispersibility (both in water and organic solvents) and stability of AuNPs in the presence of 3-APTMS and cyclohexanone is described in Chapter (IV). Further, the AuNPs suspension is converted to homogenous nanocomposite suspension with PBNPs and ruthenium bipyridyl solution [AuNPs-PBNPs-Ru(bpy)] justifying even better catalytic ability than that of HRP. The next chapter (Chapter V) deals with the use of homologous series of carbonyl group (“-C=O”) containing organic reducing agents i.e. formaldehyde (HCHO), acetaldehyde (CH₃CHO) and acetone (CH₃COCH₃) for the fabrication of 3-APTMS mediated AuNPs. The pH- and Salt- sensitivity of AuNPs has been monitored as a function of reducing agent and 3-APTMS concentration. A typical example on the role of AuNPs in homogenous catalysis during potassium ferricyanide mediated oxidation of ascorbic acid is also reported. Chapter (VI) describes the “one pot two step” rapid synthesis of trimetallic (Ag/Au/Pd) NPs utilizing 3-APTMS and formaldehyde. The synthesized trimetallic NPs behave as excellent catalyst for the reduction of PNP to PAP both in homogenous suspension and as heterogenous solid matrix. Bifunctionality of 3-APTMS has been utilized in the last chapter (VII) for the fabrication of hybrid between AuNPs and porous siloxane matrix. Solvent induces the formation of the hybrid which is mainly obtained in the case of organic

solvents. Use of water as synthesis media yields spherical AuNPs without the formation of siloxane polymer. The reversible imine linkage between 3-APTMS [$\text{NH}_2(\text{CH}_2)_3\text{Si}(\text{OMe})_3$] and acetone [$\text{CH}_3(\text{CO})\text{CH}_3$] is exploited for AuNPs synthesis both in suspension and over a solid support. AuNPs layer made over solid support is used repeatedly for the reduction of PNP in the presence of excess NaBH_4 .

The contents of the thesis have been published in *Journal of nanoscience and nanotechnology* 2014, 14, 6606, *Journal of Material Chemistry B* 2014, 2, 3383, *RSC Advances* 2014, 4, 60563, *Journal of nanoscience and nanotechnology* 2016, 16, 6155-6163, *Catalysis Science and Technology* 2016, 6, 3911.

LIST OF FIGURES

Figure No.	Figure Caption	Page No.
Figure 1.1	The Lycurgus Cup in reflected (left) and in transmitted (right) light. © Trustees of the British Museum.	2
Figure 1.2	Different shapes acquired by gold at nanoscale.	6
Figure 2.1	UV-Vis spectra recorded for the interaction between 3-GPTMS and 3-APTMS; (Left) systems containing constant concentrations of 3-GPTMS (24 mM, black line) followed by addition of varying concentration between 8–18 mM of 3-APTMS (a)–(e); (Right) systems containing constant concentrations of 3-APTMS (27 mM, black line) followed by addition of varying concentration between 9–20 mM of 3-GPTMS (a)–(e).	31
Figure 2.2	UV-Vis spectra for interaction between 3-GPTMS and 3-APTMS in the presence of tetrachloroauric acid (HAuCl ₄). Curve-1 (for both Figures) shows the absorption spectra of methanolic solution of HAuCl ₄ (0.125 mM); (Left) systems containing methanolic solutions of 3-APTMS (27 mM) treated HAuCl ₄ (red line) followed by addition of varying concentration of 3-GPTMS between 9–20 mM (a)–(e). (Right) systems containing methanolic solutions of HAuCl ₄ (0.125 mM, red line) and 3-GPTMS (24	32

mM) followed by addition of varying concentration between 8–18 mM methanolic solution of 3-APTMS (a)–(e).

- Figure 2.3** TEM images of two different sizes AuNP red (i), AuNP purple (ii). **32**
- Figure 2.4** The visual photographs of AuNPs made by using constant concentration of 3-APTMS (0.6M) and varying concentrations of 3-GPTMS (A) 1.0 M, (B) 0.75 M, and (C) 0.5 M and their dispersibility in toluene and water. The lower portion shows the UV-Vis spectra of the corresponding sols in toluene and water. **34**
- Figure 2.5** The visual photographs of AuNPs made by using constant concentration of 3-APTMS (0.2 M) and varying concentrations of 3-GPTMS (K) 1.0 M, (L) 0.75 M, and (M) 0.5 M and their dispersibility in toluene and water. The lower portion shows the UV-Vis spectra of the corresponding sols in toluene and water. **35**
- Figure 2.6** The visual photographs of AuNPs made by using constant concentration of 3-GPMTS (1.0 M) and varying concentrations of 3-APTMS (R) 0.6 M, (S) 0.4 M, and (T) 0.2 M and their dispersibility in toluene and water. The lower portion shows the UV-Vis spectra of the corresponding sols in toluene and water. **37**
- Figure 2.7** UV-Vis spectra of AuNPs in (i) toluene, (ii) ethyl-acetate, inset shows the dependence of absorption maxima (λ_{max}) on relative concentration. **38**

Figure 2.8	UV-Vis spectra of AuNPs in (i) dichloromethane, (ii) acetonitrile, inset shows the dependence of absorption maxima (λ_{\max}) on relative concentration.	38
Figure 2.9	Shows the dependence of absorption maxima (λ_{\max}) on refractive index of solvents (acetonitrile, ethylacetate, dichloromethane and toluene).	39
Figure 2.10	Shows the dependence of absorption maxima (λ_{\max}) on polarity index of solvents (toluene, dichloromethane, ethylacetate and acetonitrile).	39
Figure 2.11	Color evolutions upon addition of AuNPs to o-dianisidine- H_2O_2 system (A); Typical UV-Vis spectra of o-dianisidine H_2O_2 -AuNPs reaction system (B).	40
Figure 3.1	UV-Vis spectra showing change in λ_{\max} of AuNPs made using constant concentration of THF-HPO (11.3 mg) and varying concentrations of 3-APTMS; (i) 4mM, (ii) 6mM, (iii) 8mM, (iv) 10mM, (v) 12mM, and (vi) 14mM.	53
Figure 3.2	UV-Vis spectra showing change in λ_{\max} of AuNPs made using 3-APTMS (A=5mM) containing THF-HPO of three different concentrations [11.3 mg (black line, vii), 33.9 mg (red line, viii) and 56.5 mg (green line, ix).	54
Figure 3.3	UV-Vis spectra showing change in λ_{\max} of AuNPs made using 3-APTMS (A=10m M) containing THF-HPO of three different concentrations [11.3 mg (black line, iv), 33.9 mg (red line, x) and	54

56.5 mg (green line, xi)].

- Figure 3.4** UV-Vis spectra showing change in λ_{\max} of AuNPs made using 3-APTMS (A=14mM) containing THF-HPO of three different concentrations [11.3 mg (black line, vi), 33.9 mg (red line, xii) and 56.5 mg (green line, xiii)]. **55**
- Figure 3.5** TEM images of AuNPs made from increasing concentrations of 3-APTMS (A= 4.0mM, B= 10mM and C= 14mM) containing constant concentration of THF-HPO (11.3 mg). **55**
- Figure 3.6** (A) Time dependent UV-Vis spectrum of AuNPs made using 3-APTMS (25 mM) and THF-HPO (11.3 mg), (B) change in λ_{\max} of same AuNPs (a) on the subsequent addition of 3-APTMS; 20mL; 50 mM (b),(c) and (d). **56**
- Figure 3.7** UV-Vis spectra of AuNPs made from GBL and 3-APTMS showing change in λ_{\max} as a function of: (A) variable concentrations of 3-APTMS (xvi=0.25 M, xv=0.35 M and xvi=0.5 M) with constant concentration of GBL (40 mg); (B) variable concentrations of GBL (xvii = 50.0 mg, xviii = 60 mg and xix = 70 mg) with constant concentration of 3-APTMS (0.25 M). **56**
- Figure 3.8** Time dependent UV-Vis spectral change of o-dianisidine–H₂O₂ system catalyzed by AuNPs of variable size; (A) 10 nm (B) 25 nm and (C) 35nm. Plot-D shows the time dependent variation of absorption at 430 nm calculated from plots A, B and C **59**

respectively.

- Figure 3.9** Kinetic analysis of o-dianisidine–AuNPs–H₂O₂ system with H₂O₂ as substrate. H₂O₂ concentration is varied from to 980mM–58.9 mM. **60**
- Figure 3.10** A typical photograph showing the effect of increasing concentration of glutathione on the intensity of the color, produced due to the oxidation of o-dianisidine in o-dianisidine-H₂O₂-AuNPs reaction system. **60**
- Figure 3.11** UV-Vis spectra of o-dianisidine–H₂O₂–AuNPs system in the presence of varying concentrations of GSH (0 mM–172mM) for three sizes of AuNPs; (A) 10 nm (B) 25 nm (C) 35 nm; under the optimum conditions. **61**
- Figure 3.12** Response curves of GSH detection using o-dianisidine in the presence of AuNPs of three different sizes (D) 10 nm (E) 25 nm (F) 35 nm. Inset shows linear calibration plots for GSH analysis **61**
- Figure 3.13** UV-Vis spectra of o-dianisidine–H₂O₂–AuNPs system in the presence of varying concentration of GSH (0 mM–172mM). AuNPs of two size, (A= 35 nm,B=10 nm) were made at constant concentration of 3-APTMS (0.7). **62**
- Figure 4.1** Real time synthesis of AuNPs mediated by 3-APTMS–THF–HPO (A) and 3-APTMS–cyclohexanone (B). **78**
- Figure 4.2** UV-Vis spectra showing change in λ_{\max} of AuNPs made using a constant concentration of cyclohexanone (4.8 M) and varying **79**

concentration of 3-APTMS (i) 3 mM (ii) 4 mM (iii) 6 mM (iv) 8 mM (v) 9mM (vi) 10 mM (vii) 12 mM.

- Figure 4.3** UV-Vis spectra showing change in λ_{\max} of AuNPs made using (A) constant concentration of 3-APTMS (10 mM) and varying cyclohexanone concentration (i) 1.0 M, (ii) 1.5 M, (iii) 2.0 M, (iv) 3.0 M (v) 4.0 M; (B) constant concentration of 3-APTMS (5 mM) and varying cyclohexanone concentration; (i) 4.0 M (ii) 5.0 M (iii) 6.0 M (iv) 7.0 M (v) 8.0 M. **80**
- Figure 4.4** TEM images of AuNPs made using cyclohexanone (4.8 M) and 3-APTMS (8mM). **80**
- Figure 4.5** TEM images of AuNPs made using cyclohexanone (4.8 M) and 3-APTMS (10 mM). **81**
- Figure 4.6** TEM images of AuNPs made using cyclohexanone (4.8 M) and 3-APTMS (12 mM). **81**
- Figure 4.7** TEM images of AuNPs made using cyclohexanone (4.8 M) and 3-APTMS (15 mM). **82**
- Figure 4.8** UV-Vis spectra of AuNPs and their dispersibility in DCM, methanol and water, made using constant concentration of (A) cyclohexanone (4.8 M) and varying concentrations of 3-APTMS: (g) 5mM, (h) 7 mM, and (i) 9 mM; **83**
- Figure 4.9** UV-Vis spectra of AuNPs and their dispersibility in DCM, methanol and water, made using constant concentration of cyclohexanone (3.8 M) and varying concentrations of 3-APTMS: **84**

(j) 5 mM, (k) 7 mM, and (l) 9 mM.

- Figure 4.10** UV-Vis spectra of AuNPs and their dispersibility in DCM, methanol and water, made using constant concentration of 3-APTMS (10 mM) and varying concentrations of cyclohexanone: (m) 0.9 M, (n) 1.8 M, and (o) 3.8 M. Images of corresponding AuNPs sol in the same solvents are shown as an inset to the image. **85**
- Figure 4.11** UV-Vis spectra of AuNPs in (i) acetonitrile (ii) dichloromethane. Inset shows the dependence of absorption maxima (λ_{\max}) on relative concentration. **85**
- Figure 4.12** UV-Vis spectra of AuNPs in (i) Ethyl acetate (ii) water. Inset shows the dependence of absorption maxima (λ_{\max}) on relative concentration. **86**
- Figure 4.13** Dependence of λ_{\max} on polarity index (i) and refractive index (ii). **86**
- Figure 4.14** UV-Vis spectra of o-dianisidine–H₂O₂ system catalyzed by AuNPs, fabricated using different 3-APTMS concentration, in methanol (A and B) acetonitrile (C and D), justifying the role of functional ability. **87**
- Figure 4.15** UV-Vis spectra of AuNPs (i), PBNPs–AuNPs (ii), PBNPs–AuNPs–Ru(bpy) (iii). Inset shows the visual images of the same. **89**
- Figure 4.16** UV-Vis spectra of the o-dianisidine–H₂O₂ system catalyzed by AuNPs (i), PBNP-AuNPs (ii), and PBNP-AuNPs-Ru(bpy) (iii). **90**

- Figure 4.17** Kinetic analysis of o-dianisidine–H₂O₂ system catalyzed by AuNPs (iv), PBNPs–AuNPs and PBNPs–AuNPs–Ru(bpy) (v). **90**
- Figure 4.18** Response curve for glucose detection using glucose oxidase catalyzed formation of H₂O₂ monitored by PBNP–AuNP–Ru(bpy)–o-dianisidine system; inset to [C] shows linear calibration plot for glucose and images show colour change as a function of glucose concentrations. **92**
- Figure 4.19** Cyclic voltammograms of PB (a), PB–AuNP1 (b) and PB–AuNP2 (c) in 0.1 M phosphate buffer of pH 7.0, containing 0.5 M KCl at the scan rates of 0.01, 0.02, 0.035, 0.050, 0.070, 0.10, 0.15, 0.20, 0.25, 0.30, 0.35, 0.40, 0.45, 0.50 V s⁻¹. **93**
- Figure 4.20** Show the plot of anodic and cathodic current density vs scan rate (i) and square root of scan rate (ii) respectively **93**
- Figure 4.21** Cyclic voltammograms of PB, PB–AuNP1 and PB–AuNP2 in absence (1) and the presence (2) of 2 mM H₂O₂ in 0.1 M phosphate buffer of pH 7.0, containing 0.5 M KCl at the scan rate of 0.01 V s⁻¹. **94**
- Figure 4.22** Amperometric response of H₂O₂ analysis at 0.05 V vs. Ag/AgCl in 0.1 M phosphate buffer of pH 7.0, containing 0.5 M KCl, inset to [3] shows the linear range of calibration curves for PB (a), PB–AuNP1(b) and PB–AuNP2(c). **95**
- Figure 4.23** Dispersibility of AuNPs made using 3-APTMS and THF-HPO in water (a) methanol (b) dichloromethane and toluene (d). **98**

Figure 5.1	TEM image (left) and diffraction pattern(right) of AuNPs made using 3-APTMS and formaldehyde.	108
Figure 5.2	TEM image (left) and diffraction pattern(right) of AuNPs made using 3-APTMS and acetaldehyde.	108
Figure 5.3	TEM image (left) and diffraction pattern(right) of AuNPs made using 3-APTMS and acetone.	109
Figure 5.4	TEM image (left) and diffraction pattern(right) of AuNPs made using 3-APTMS and t-butyl methyl ketone.	109
Figure 5.5	UV-Vis spectra displaying a comparison between peroxidase mimetic ability of AuNPs made using 3-APTMS and Formaldehyde (black line), acetaldehyde (red line), acetone (green line) and t-butylmethylketone (blue line).	111
Figure 5.6	Image showing catalytic behavior for solutions made using formaldehyde (P'), acetaldehyde (Q') and non catalytic behavior for the solution made using acetone (R'), t-butyl methyl ketone (S')	112
Figure 5.7	UV-Vis spectra displaying the effect of pH on AuNPs made by using 3-APTMS (0.2 M) and (A) formaldehyde (B) acetaldehyde and (C) acetone. Inset shows the change in wavelength (λ_{\max}) with pH of the buffering media (k = water, l = 8, m = 7, n = 6, o = 5).	113
Figure 5.8	UV-Vis spectra displaying the effect of pH on AuNPs made by using formaldehyde and 3-APTMS (A) 0.1 M (B) 0.2 M and (C)	114

0.4 M. Inset shows the change in wavelength (λ_{\max}) with pH of the buffering media (k = water, l = 8, m = 7, n = 6, o = 5).

- Figure 5.9** UV-Vis spectra displaying the effect of salt concentration on AuNPs made by using formaldehyde and 3-APTMS (A) 0.1 M (B) 0.2 M and (C) 0.4 M. Insets show the change in wavelength (λ_{\max}) with salt concentration (k = water, l = 0.1 M, m = 0.2 M, n = 0.5 M, o = 1.0 M). **115**
- Figure 5.10** Cyclic voltammogram of potassium ferricyanide in absence (A) and the presence (B) of AuNPs in 0.1 M phosphate buffer of pH 7 containing 0.1 M KCl at the scan rate of 10, 20, 35, 50, 100, 150, 200, 250, 300, 350, 400, 450, and 500 V s⁻¹. **116**
- Figure 5.11** (A) shows the plot of anodic and cathodic current density versus scan rate in absence (1) and the presence (2) of AuNPs. (B) shows the plot of anodic and cathodic current density versus square root of scan rate in absence (1) and the presence (2) of AuNPs. **116**
- Figure 5.12** Show the oxidation of ascorbic acid using potassium ferricyanide as mediator in absence (A) and the presence (B) of AuNPs in 0.1 M phosphate buffer containing 0.1 M KCl at the scan rate of 10mVs⁻¹. **117**
- Figure 6.1** UV-Vis spectra of 10.7 mM PdCl₂ (i), 10.7 mM PdCl₂ and 0.5M 3-APTMS (ii), 10.7 mM PdCl₂, 0.5 M 3-APTMS and 1.9 M formaldehyde (iii) and PdNPs formed (iv). **130**

Figure 6.2	UV-Vis spectra of sequentially (A) and simultaneously (B) made AuPd bimetallic nanoparticles.	130
Figure 6.3	TEM images and diffraction pattern of Au@Pd (A-i, B-i) and AuPd (A-ii, B-ii).	131
Figure 6.4	Typical UV-Vis spectra of PNP and PAP (left side) and time dependent reduction of PNP (i) in the presence of excess NaBH ₄ and (Au@Pd) (ii), (AuPd) (iii) [as catalyst]	131
Figure 6.5	UV-Vis spectra of PdNPs, (AuPd)NPs and Ag@(AuPd)NPs	133
Figure 6.6	UV-Vis spectra of (A) Bimetallic (PdAu) NPs made at increasing concentration of Au ³⁺ and (B) Trimetallic Ag@(PdAu) NPs made by adding constant concentration of Ag ⁺ to (PdAu) made using different Au ³⁺ concentration.	133
Figure 6.7	TEM image (left) and diffraction pattern (right) of PdNPs.	134
Figure 6.8	TEM image (left) and diffraction pattern (right) of (PdAu)NPs.	134
Figure 6.9	TEM image (left) and diffraction pattern (right) of Ag@(PdAu)NPs.	135
Figure 6.10	XPS spectra of Pd in PdNPs.	135
Figure 6.11	XPS spectra of Pd (left) and Au (right) in PdAu bimetallic NPs.	136
Figure 6.12	XPS spectra of Pd (left), Ag (middle) and Au (right) in Ag@PdAu trimetallic NPs.	136
Figure 6.13	Typical UV-Vis spectra for reduction of PNP to PAP (left).	137

Pictorial representation for showing transition from yellow color of PNP to colorless PAP.

- Figure 6.14** Plot of $\ln(A_{400})$ versus time for the reduction of 4-NP for Ag@(AuPd)NPs (left), (AuPd)NPs (middle) and PdNPs (right). **137**
- Figure 6.15** Pictorial representation for the conversion of Homogenous suspension of 3-APTMS and formaldehyde mediated trimetallic NPs to heterogenous solid matrix in the presence of HCl. **139**
- Figure 6.16** UV-Vis spectra displaying the decrease in absorbance value for the peak at 400nm corresponding to PNP in the presence of powder catalyst and excess NaBH_4 . Inset shows the image for the same. **140**
- Figure 6.17** UV-Vis spectra of showing the stability of AuNPs (A) and AgNPs (B) in the presence of HCl relative to water. **140**
- Figure 7.1** Pictorial representation of AuNPs made using 3-APTMS and acetone in (a) water, (b) methanol, (c) acetone and (d) chloroform. **155**
- Figure 7.2** UV-Vis spectra of AuNPs made using 3-APTMS and acetone in (a) water, (b) methanol, (c) acetone and (d) chloroform. **156**
- Figure 7.3** SEM images of AuNPs made in water (a) and acetone (b). **156**
- Figure 7.4** SEM images of “Siloxane-AuNPs” hybrid made using (A) chloroform and (B) acetone. The images clearly display the porosity in hybrid structures. **157**

Figure 7.5	AFM (a) and SEM (b) images of AuNPs made in chloroform showing organized wire-like structures.	157
Figure 7.6	TEM images of AuNPs made in water (a) and acetone (b).	158
Figure 7.7	HAADF-STEM-EDS images showing Si mapping images for AuNPs made using 3-APTMS and acetone (both as solvent and mild reducing agent).	159
Figure 7.8	HAADF-STEM-EDS images showing (Si + Au) mapping images for AuNPs made using 3-APTMS and acetone (both as solvent and mild reducing agent).	159
Figure 7.9	HAADF-STEM-EDS images showing AuNPs made using 3-APTMS and acetone (both as solvent and mild reducing agent): A) Si mapping; B) Si+Au mapping ; and C) Au mapping. (Enlargements of the same part of each image)	160
Figure 7.10	UV-Vis spectra of siloxane polymer (a) and “(Au-siloxane _{homo}) _{seq} ” NPs (b).	160
Figure 7.11	SEM images of siloxane polymer (a) and “Au@siloxane _{hetero} ” NPs(b).	161
Figure 7.12	Cyclic voltammogramme of “siloxane-Au _{sim} ” NPs showing increasing current trend at a scan rate of 10mV s ⁻¹ .	162
Figure 7.13	Cyclic voltammogramme of “Au@siloxane _{homo} ” NPs showing constant current with successive cycles at a scan rate of 10mVs ⁻¹ .	162
Figure 7.14	Cyclic voltammogramme of (FeCN ₆) ^{3-/4-} in 0.1M phodphate buffer (pH=7) containing 0.5M KCl in blank (A) and modified	163

electrode (B) at a scan rate of 10mVs^{-1} .

- Figure 7.15** Plot of anodic (i_{pa}) and cathodic (i_{pc}) current density vs scan rate in blank (A) and modified electrode (B) (Left, C). Plot of anodic (i_{pa}) and cathodic current density (i_{pc}) vs square root of scan rate in blank (A) and over modified electrode (B) (Right, D). **163**
- Figure 7.16** Picture presenting change of color from yellow (PNP) to colorless (PAP) in the presence of excess NaBH_4 and “ $\text{Au@siloxane}_{\text{hetero}}$ ” solid catalyst. **164**
- Figure 7.17** Typical UV-Vis spectra for reduction of PNP over catalyst of interest with an excess amount of NaBH_4 (a). Plot of $\ln A_{400}$ vs time for the reduction of PNP using “ $\text{Au@siloxane}_{\text{hetero}}$ ”NPs (b). **164**
- Figure 7.18** UV-Vis spectra for the competitive ability of different AuNPs towards peroxidase mimetic ability. **165**

LIST OF TABLES

Table No.	Table Caption	Page No.
Table 2.1	Concentrations of the reagents used during the synthesis of AuNPs by the action of 3-GPTMS on 3-APTMS capped Au ³⁺ .	29
Table 2.2	Dispersibility of nanoparticles having constant concentrations of 3-APTMS (3 M) and varying concentrations of 3-GPTMS.	34
Table 2.3	Dispersibility of nanoparticles having constant concentrations (limiting) of 3-APTMS (1 M) in presence of varying concentrations of 3-GPTMS.	35
Table 2.4	Dispersibility of nanoparticles having varying concentrations of 3-APTMS and constant concentrations of 3-GPTMS (4 M).	37
Table 3.1	3-APTMS and THF-HPO mediated synthesis of AuNPs showing change in $\ln \max$ as a function of reactant concentrations	49
Table 3.2	Effect of GBL on 3-APTMS-mediated synthesis of AuNPs	50
Table 5.1	A comparative study on the peroxidase mimetic ability of AuNPs made from the use of 3-APTMS capped Au ³⁺ and various organic reducing agents (P for formaldehyde; Q for acetaldehyde; R for acetone; and S for t-butylmethyl ketone).	111
Table 5.2	A comparative study on the peroxidase mimetic ability of solutions made from the use of 3-APTMS and various organic reducing agents (P' for formaldehyde; Q' for acetaldehyde; R' for acetone; and S' for t-butylmethyl ketone) in absence of Au ³⁺ .	112

Table 5.3	pH-Sensitivity of AuNPs, made using 3-APTMS (0.2 M) and Formaldehyde, Acetaldehyde or Acetone.	113
Table 5.4	Salt and pH sensitivity of AuNPs made using formaldehyde and varying 3-APTMS concentration.	115
Table 6.1	Concentration of different constituents utilized during the synthesis of PdNPs, (PdAu)NPs and Ag@(PdAu)NPs.	126
Table 6.2	d-Spacing values for rings obtained in diffraction pattern of synthesized nanoparticles.	141
Table 6.3	Binding Energy data for individual components of PdNPs, (PdAu)NPs and Ag@(PdAu).	143
Table 6.4	A comparative study on the catalyzing ability of nanoparticles [Pd, (PdAu) and Ag@(PdAu)] during the reduction of PNP (0.015M) to PAP in the presence of excess NaBH ₄ (0.05 M).	145

LIST OF ABBREVIATIONS

NPs	: Nanoparticles
MNPs	: Metal Nanoparticles
AuNPs	: Gold Nanoparticles
NaBH ₄	: Sodium Borohydride
HAuCl ₄	: Chloroauric acid
SPR	: Surface Plasmon Resonance
Con A	: Concanavalin A
FRET	: Fluorescence Resonance Energy Transfer
CdSe	: Cadmium Selenide
QDs	: Semiconductor quantum dots
H ₂ O ₂	: Hydrogen peroxide
ODA	: o-Dianisidine
TMB	: 3,3,5,5-Tetramethylbenzidine
HRP	: Horseradish Peroxidase
PNP	: para-Nitrophenol
PAP	: para-Aminophenol
3-APTMS	: 3-Aminopropyltrimethoxysilane
3-GPTMS	: 3-Glycidoxypropyltrimethoxysilane
THF-HPO	: Tetrahydrofuranhydroperoxide
AgNPs	: Silver nanoparticles
PdNPs	: Palladium nanoparticles

GBL	: γ - Butyrolactone
THF-HPO	: Tetrahydrofuran hydroperoxide
GSH	: Glutathione
K _m	: Michaelis Menten constant
V _{max}	: Maximal reactionvelocity
Ru(bpy)	: Ruthenium bipyridyl
PBNPs	: Prussian Blue nanoparticles
h	: Hours
TEM	: Transmission Electron Microscopy
SEM	: Scanning Electron Microscopy
AFM	: Atomic Force Microscopy
SAED	: Surface Area Electron Diffraction
IPTMS	: N-isopropylidene-3-aminopropyltrimethoxysilane
TIPS	: Triisopropylsilane
AuNWs	: Gold nanowires
K _{app}	: Apparent rate constant
GCE	: Glassy Carbon Electrode
HAADF-STEM-EDS	: High-angle annular dark field- Scanning transmission electron microscopy-Energy dispersive X-ray spectroscopy
t-DMK	: t-Butyldimethylketone
TMSPdien	: 3-(trimethoxysilylpropyl)diethylenimine
HCl	: Hydrochloric acid
HCHO	: Formaldehyde

min	: Minutes
CV	: Cyclic Voltammetry
CMC	: Critical Micellar Concentration
nm	: nanometer
DCM	: Dichloromethane